1-1-2004

Stationkeeping of an L_2 Libration Point Satellite with θ-D Technique

Ming Xin

S. N. Balakrishnan
Missouri University of Science and Technology, bala@mst.edu

Hank Pernicka
Missouri University of Science and Technology, pernicka@mst.edu

Michael W. Dancer

Recommended Citation

M. Xin et al., "Stationkeeping of an L_2 Libration Point Satellite with θ-D Technique," *Proceedings of the 2004 American Control Conference*, Institute of Electrical and Electronics Engineers (IEEE), Jan 2004.

Stationkeeping of an L_2 Libration Point Satellite with $\theta - D$ Technique

Ming Xin[+], M. W. Dancer[++], S.N. Balakrishnan[**], H.J. Pernicka[**]
xin@umr.edu , mdancer@umr.edu, bala@umr.edu , pernicka@umr.edu
Department of Mechanical and Aerospace Engineering
University of Missouri-Rolla, Rolla, MO 65409-0050

Abstract-**A new method for L_2 libration-point orbit stationkeeping is proposed in this paper using continuous thrust. The circular restricted three-body problem with Sun and Earth as the two primaries is considered. The unstable orbit about the L_2 libration-point requires stationkeeping maneuvers to maintain the nominal path. In this study, an approach, called the "$\theta - D$ technique," based on optimal control theory gives a closed-form suboptimal feedback solution to solve this nonlinear control problem. In this approach the Hamiltonian-Jacobi-Bellman (HJB) equation is solved approximately by adding some perturbations to the cost function. The controller is designed such that the actual trajectory tracks a predetermined reference orbit with good accuracy. Numerical results employing this method demonstrate the potential of this method.**

I. INTRODUTION

There has been active interest in recent years in missions utilizing trajectories near libration points. Libration points or Lagrangian points are equilibrium points where in the restricted three-body problem the gravitational and centrifugal forces acting on the third body cancel. Spacecraft in orbits near libration points offer valuable opportunities for investigations concerning solar and heliospheric effects on planetary environments. Preliminary trajectory analysis and design are often carried out in the context of the circular restricted three-body problem (CR3BP) with the Sun and the Earth as the primary gravitational bodies. The framework allows the identification of mission-enabling trajectories such as halo orbits around the libration points. A number of missions have already incorporated Lissajous or halo orbits about the L_1 libration point as part of the trajectory design such as ISEE-3 (1978), SOHO (1995) and ACE (1997).

It is well-known [1] that the orbits about the collinear libration points are unstable. Spacecraft moving on these paths must use some form of trajectory control to remain close to their nominal orbit. A number of stationkeeping strategies have been proposed since the late 1960s [2]. In 1970, Farquhar [2] presented several possible methods for libration point orbits. Breakwell [3] in 1974 published his approach for stationkeeping spacecraft on halo orbits around the Earth-Moon L_2 libration point. Simo et al. in 1986 [4] employed Floquet and invariant manifold theories to develop a loose control for halo-type orbits. In 1993, Howell and Pernicka [5], modified Dwivedi's [6] method and successfully used it to control the spacecraft trajectory near the nominal path. In a 1996 paper, Cielaszyk and Wie [7] utilized a disturbance accommodating, linear state feedback controller based on LQR technique for the computation of a trajectory about the Earth-Moon L_2 libration point that can be used as a fuel-efficient nominal path. Dunham and Roberts [8] in 2001 gave a detailed review of the stationkeeping strategies used on the three major libration-point orbit missions, ISEE-3, SOHO and ACE. A tight control technique was discussed for ISEE-3 and an orbital energy balancing based loose control for SOHO and ACE demonstrate a significant improvement in expenditures of fuel. In [9], Rahmani et al. used optimal control theory to develop a new stationkeeping method for active control of spacecraft on a reference trajectory. The variation of extremals, an iterative numerical technique, is used to calculate the optimal control acceleration.

In this paper, we propose a new method, the "$\theta - D$ technique," to design a stationkeeping strategy based upon optimal control theory. This strategy uses nonlinear equations of spacecraft in the scenario of the CR3BP. An approximately suboptimal closed-form feedback controller can be obtained using this approach. The nominal trajectory is first calculated using the method in [10]. The $\theta - D$ controller is then applied to drive the spacecraft to this reference trajectory. Numerical results are presented to demonstrate the effectiveness of this method.

II. CIRCULAR RESTRICTED THREE-BODY PROBLEM

Figure 1 shows the geometry of the restricted three-body problem used in this study. Two of the libration points, L_1 and L_2 are shown. A rotating reference frame is defined with origin at the libration point of interest and at the barycenter of the two-body system. In both cases, the $\hat{\mathbf{x}}$ unit vector is directed from the larger primary toward the smaller primary. The $\hat{\mathbf{y}}$ unit vector is defined normal to the $\hat{\mathbf{x}}$ vector, within the plane of the primaries' orbit, and along the prograde rotational direction. The $\hat{\mathbf{z}}$ unit vector then completes the right-handed frame and is thus normal to the plane of the primaries' orbit. If the spacecraft is located by a position vector $\mathbf{r}$ with base point at the barycenter using coordinates x, y, and z with respect to the rotating frame, then the well-known equation of motion for Circular Restricted Three-Body Problem (CR3BP) are given by

$$\ddot{x} - 2\dot{y} - x = -\frac{(1-\mu)(x+\mu)}{r_1^3} - \frac{\mu[x-(1-\mu)]}{r_2^3} \quad (1)$$

$$\ddot{y} + 2\dot{x} - y = -\frac{(1-\mu)y}{r_1^3} - \frac{\mu y}{r_2^3} \quad (2)$$

$$\ddot{z} = -\frac{(1-\mu)z}{r_1^3} - \frac{\mu z}{r_2^3} \quad (3)$$

**: Professor, contact person +: Postdoctoral research fellow
++: Undergraduate Student

where

$r_1=(x+\mu)\hat{x}+y\hat{y}+z\hat{z}, r_2=(x-(1-\mu))\hat{x}+y\hat{y}+z\hat{z}, r=x\hat{x}+y\hat{y}+z\hat{z}$ (4)

where μ is the ratio of the smaller primary mass to the sum of the masses of both primaries, and r_1 and r_2 are the distances from the larger and smaller primary to the spacecraft, respectively.

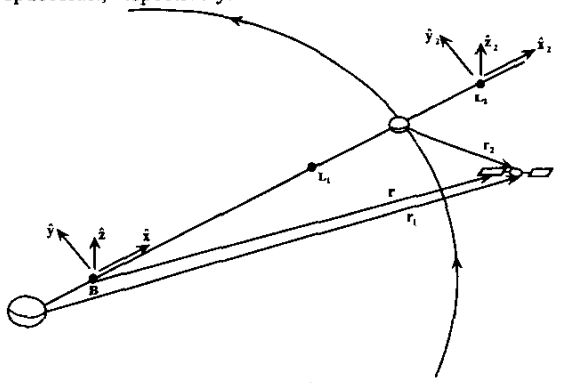

Fig. 1: Basic Geometry of the Restricted Three-Body Problem

For the Sun-Earth/Moon system, $\mu=3.0404234945077\times10^{-6}$.

The above equations are expressed in nondimensional form. We define the distance between the two primaries as the unit of length and denote it as R and the time in units $1/n$, where n is the mean motion. For the Sun-Earth system, we have

$R=1.4959787066\times10^{8}$ km, $n=1.990986606\times10^{-7}$ rad/sec

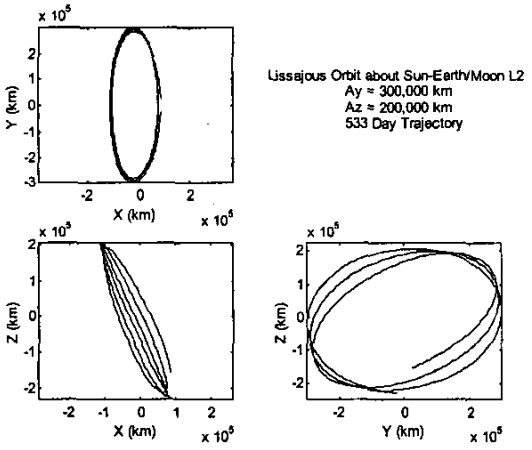

Fig. 2: Nominal Lissajous Orbit about L_2 Libration Point

The nominal Lissajous trajectory used in this study was computed about the Sun-Earth/Moon L_2 libration point and is shown in Fig. 2 in a three-view orthographic projection. This orbit has approximate amplitudes $A_y \cong 300{,}000$ km and $A_z \cong 200{,}000$ km. The 533 day trajectory was numerically integrated in the circular restricted three-body problem using the method described in reference [10].

In the next section, a new nonlinear optimal control technique is presented as a stationkeeping method.

III. SUMMARY OF THE θ-D CONTROL METHOD

In this paper the state feedback control problem is restricted for the class of nonlinear time-invariant systems described by

$$\dot{x}=f(x)+\mathbf{g}u \tag{5}$$

with the cost function:

$$J=\frac{1}{2}\int_0^\infty [x^T\mathbf{Q}x+u^T\mathbf{R}u]dt \tag{6}$$

where $x\in\Omega\subset\mathbf{R}^n, f\in\mathbf{R}^n, \mathbf{g}\in\mathbf{R}^{n\times m}, u\in\mathbf{R}^m, \mathbf{Q}\in\mathbf{R}^{n\times n}, \mathbf{R}\in\mathbf{R}^{m\times m}$.

Ω is a compact set in $\mathbf{R}^n$; $\mathbf{f}(x)$ is continuously differentiable in x and $\mathbf{g}$ is a constant matrix; The condition $f(\mathbf{0})=\mathbf{0}$ is assumed in order to have the system at equilibrium when it is at the origin. $\mathbf{Q}$ is assumed to be a positive semi-definite constant matrix and $\mathbf{R}$ is assumed to be a positive-definite constant matrix.

The optimal solution of the infinite-horizon nonlinear regulator problem can be obtained by solving the Hamilton-Jacobi-Bellman (HJB) partial differential equation [11]:

$$\frac{\partial V^T}{\partial x}f(x)-\frac{1}{2}\frac{\partial V^T}{\partial x}\mathbf{g}\mathbf{R}^{-1}\mathbf{g}^T\frac{\partial V}{\partial x}+\frac{1}{2}x^T\mathbf{Q}x=0 \tag{7}$$

where $V(x)$ is the optimal cost, i.e.

$$V(x)=\min_u\frac{1}{2}\int_0^\infty (x^T\mathbf{Q}x+u^T\mathbf{R}u)dt \tag{8}$$

It is assumed that $V(x)$ is continuously differentiable and $V(x)>0$ with $V(\mathbf{0})=0$.

The necessary condition for optimality leads to

$$\mathbf{u}=-\mathbf{R}^{-1}\mathbf{g}^T\frac{\partial V}{\partial x} \tag{9}$$

The HJB equation is extremely difficult to solve. The following approximations are made.

Consider perturbations added to the cost function:

$$J=\frac{1}{2}\int_0^\infty [x^T(\mathbf{Q}+\sum_{i=1}^{\infty}\mathbf{D}_i\theta^i)x+u^T\mathbf{R}u]dt \tag{10}$$

Rewrite the original state equation as:

$$\dot{x}=f(x)+\mathbf{g}u=F(x)x+\mathbf{g}u=\left\{\mathbf{A}_0+\theta\left[\frac{\mathbf{A}(x)}{\theta}\right]\right\}x+\mathbf{g}u \tag{11}$$

where θ is an intermediate variable; $\mathbf{A}_0$ is a constant coefficient matrix such that $(\mathbf{A}_0,\mathbf{g})$ is a stabilizable pair and $[\mathbf{A}_0+\mathbf{A}(x),\mathbf{g}]$ is pointwise controllable.

Define $$\lambda=\frac{\partial V}{\partial x} \tag{12}$$

By using (12) in (7) and using the perturbed cost function, the HJB equation (7) becomes

$$\lambda^T f(x)-\frac{1}{2}\lambda^T\mathbf{g}\mathbf{R}^{-1}\mathbf{g}^T\lambda+\frac{1}{2}x^T(\mathbf{Q}+\sum_{i=1}^{\infty}\mathbf{D}_i\theta^i)x=0 \tag{13}$$

Assume a power series expansion of λ as

$$\lambda=\sum_{i=0}^{\infty}\mathbf{T}_i\theta^i x \tag{14}$$

where $\mathbf{T}_i$ are to be determined and assumed to be symmetric.

Substitute equation (14) into equation (13) and equate the coefficients of powers of θ to zero to get the following equations:

$$\mathbf{T}_0\mathbf{A}_0 + \mathbf{A}_0{}^T\mathbf{T}_0 - \mathbf{T}_0\mathbf{g}\mathbf{R}^{-1}\mathbf{g}^T\mathbf{T}_0 + \mathbf{Q} = 0 \quad (15)$$

$$\mathbf{T}_1(\mathbf{A}_0 - \mathbf{g}\mathbf{R}^{-1}\mathbf{g}^T\mathbf{T}_0) + (\mathbf{A}_0{}^T - \mathbf{T}_0\mathbf{g}\mathbf{R}^{-1}\mathbf{g}^T)\mathbf{T}_1 = \frac{\mathbf{T}_0\mathbf{A}(x)}{\theta} - \frac{\mathbf{A}^T(x)\mathbf{T}_0}{\theta} - \mathbf{D}_1 \quad (16)$$

$$\vdots$$

$$\mathbf{T}_n(\mathbf{A}_0 - \mathbf{g}\mathbf{R}^{-1}\mathbf{g}^T\mathbf{T}_0) + (\mathbf{A}_0{}^T - \mathbf{T}_0\mathbf{g}\mathbf{R}^{-1}\mathbf{g}^T)\mathbf{T}_n = -\frac{\mathbf{T}_{n-1}\mathbf{A}(x)}{\theta} - \frac{\mathbf{A}^T(x)\mathbf{T}_{n-1}}{\theta} + \sum_{j=1}^{n-1}\mathbf{T}_j\mathbf{g}\mathbf{R}^{-1}\mathbf{g}^T\mathbf{T}_{n-j} - \mathbf{D}_n \quad (17)$$

Since the right hand side of equations (16)-(17) involve x and θ, $\mathbf{T}_i$ would be the function of x and θ. Thus it is denoted as $\mathbf{T}_i(x,\theta)$.

Control can be obtained in terms of the power series for λ

$$u = -\mathbf{R}^{-1}\mathbf{g}^T\lambda = -\mathbf{R}^{-1}\mathbf{g}^T\sum_{i=0}^{\infty}\mathbf{T}_i(x,\theta)\theta^i x \quad (18)$$

Construct the following expression for $\mathbf{D}_i$:

$$\mathbf{D}_1 = k_1 e^{-l_1 t}\left[-\frac{\mathbf{T}_0\mathbf{A}(x)}{\theta} - \frac{\mathbf{A}^T(x)\mathbf{T}_0}{\theta}\right] \quad (19)$$

$$\vdots$$

$$\mathbf{D}_n = k_n e^{-l_n t}\left[-\frac{\mathbf{T}_{n-1}\mathbf{A}(x)}{\theta} - \frac{\mathbf{A}^T(x)\mathbf{T}_{n-1}}{\theta} + \sum_{j=1}^{n-1}\mathbf{T}_j\mathbf{g}\mathbf{R}^{-1}\mathbf{g}^T\mathbf{T}_{n-j}\right] \quad (20)$$

where k_i and $l_i > 0, i = 1,\cdots n$ are adjustable design parameters. $\mathbf{D}_i$ is chosen such that

$$\frac{\mathbf{T}_{i-1}\mathbf{A}(x)}{\theta} - \frac{\mathbf{A}^T(x)\mathbf{T}_{i-1}}{\theta} + \sum_{j=1}^{i-1}\mathbf{T}_j\mathbf{g}\mathbf{R}^{-1}\mathbf{g}^T\mathbf{T}_{i-j} - \mathbf{D}_i = \varepsilon_i(t)\left[-\frac{\mathbf{T}_{i-1}\mathbf{A}(x)}{\theta} - \frac{\mathbf{A}^T(x)\mathbf{T}_{i-1}}{\theta} + \sum_{j=1}^{i-1}\mathbf{T}_j\mathbf{g}\mathbf{R}^{-1}\mathbf{g}^T\mathbf{T}_{i-j}\right], i = 1,\cdots n \quad (21)$$

where $\varepsilon_i(t) = 1 - k_i e^{-l_i t}$ is a small number and can be used to suppress the large value from propagating in equations (16) through (17) if initial large states result in large $A(x)$ [12]. $\varepsilon_i(t)$ is chosen to satisfy some conditions required in the proof of convergence and stability of the above algorithm [12]. On the other hand, the exponential term $e^{-l_i t}$ with $l_i > 0$ is used to let the perturbation terms in the cost function and HJB equation diminish as time evolves. Another purpose of $\mathbf{D}_i$ is to allow flexibility to modulate the system transient performance by tuning the parameters of k_i and l_i in the $\mathbf{D}_i$.

The steps of applying the $\theta - D$ method are summarized as follows:

1) Solve the algebraic Riccati equation (15) to get $\mathbf{T}_0$ once $\mathbf{A}_0, \mathbf{g}$, $\mathbf{Q}$ and $\mathbf{R}$ are determined. Note that the resulting $\mathbf{T}_0$ is a positive-definite constant matrix.

2) Solve the Lyapunov equation (16) to get $\mathbf{T}_1(x,\theta)$. Note that it is a linear equation in terms of $\mathbf{T}_1$ and an interesting property of this equation and Eq. (17) is that the coefficient matrices $\mathbf{A}_0 - \mathbf{g}\mathbf{R}^{-1}\mathbf{g}^T\mathbf{T}_0$ and $\mathbf{A}_0{}^T - \mathbf{T}_0\mathbf{g}\mathbf{R}^{-1}\mathbf{g}^T$ are constant matrices. Assume that $\mathbf{A}_{c_0} = \mathbf{A}_0 - \mathbf{g}\mathbf{R}^{-1}\mathbf{g}^T\mathbf{T}_0$. Through linear algebra, Eq. (16) can be brought into a form like $\hat{\mathbf{A}}_0 Vec(\mathbf{T}_1) = Vec[\mathbf{Q}_1(x,\theta,t)]$ where $\mathbf{Q}_1(x,\theta,t)$ is the right-hand side of the equation (16); $Vec(\mathbf{M})$ denotes stacking the elements of matrix $\mathbf{M}$ by rows in a vector form; $\hat{\mathbf{A}}_0 = \mathbf{I}_n \otimes \mathbf{A}_{c_0}^T + \mathbf{A}_{c_0}^T \otimes \mathbf{I}_n$ is a constant matrix and the symbol $\otimes$ denotes the Kronecker product. The resulting solution of $\mathbf{T}_1$ can be written as a closed-form expression $Vec(\mathbf{T}_1) = \hat{\mathbf{A}}_0^{-1} Vec[\mathbf{Q}_1(x,\theta,t)]$.

3) Solve the equations (17) by following the similar procedure to Step 2. For most of the problems, the first three terms, i.e. $\mathbf{T}_0, \mathbf{T}_1$ and $\mathbf{T}_2$, in the control equation (18) are sufficient to achieve satisfactory performance. More terms could be added if needed.

As can be seen, closed-form solutions for $\mathbf{T}_2,\cdots,\mathbf{T}_n$ can be obtained with just one matrix inverse operation. The expression of $\mathbf{Q}_i(x,\theta,t)$ on the right hand side of the equations is already known and needs simple matrix multiplications and additions.

Remark 3.1: θ is just an intermediate variable. The introduction of θ is for the convenience of writing λ as a power series expansion. It gets cancelled when $\mathbf{T}_i(x,\theta)$ multiply θ^i in the final control calculations, i.e. Eq. (18).

Remark 3.2: The selection of k_i and l_i parameters can be done systematically [13] by applying the least square curve fitting to find k_i and l_i such that the errors between $\sigma_{\max}\left[\sum_{i=0}^{n}\mathbf{T}_i(x,\theta)\right]$ and $\sigma_{\max}[\boldsymbol{P}(x)]$ are minimized, where $\boldsymbol{P}(x)$ is the solution of the state dependent Riccati equation:

$$\boldsymbol{F}^T(x)\boldsymbol{P}(x) + \boldsymbol{P}(x)\boldsymbol{F}(x) - \boldsymbol{P}(x)\boldsymbol{g}\boldsymbol{R}^{-1}\boldsymbol{g}^T\boldsymbol{P}(x) + \boldsymbol{Q} = \boldsymbol{0} \quad (22)$$

In summary, the $\theta - D$ controller obtains a closed-form suboptimal feedback solution to the nonlinear optimal regulator problem if finite terms in control are taken.

IV. $\theta - D$ CONTROLLER DESIGN FOR STATIONKEEPING OF AN L_2 LIBRATION POINT SATELLITE

Write the CR3BP Eqs. (1)-(3) in the state space form with controls incorporated:

$$\dot{x}_1 = x_2 \quad (23)$$

$$\dot{x}_2 = 2x_4 + x_1 - \frac{(1-\mu)(x_1+\mu)}{r_1^3} - \frac{\mu[x_1-(1-\mu)]}{r_2^3} + u_1 \quad (24)$$

$$\dot{x}_3 = x_4 \quad (25)$$

$$\dot{x}_4 = -2x_2 + x_3 - \frac{(1-\mu)x_3}{r_1^3} - \frac{\mu x_3}{r_2^3} + u_2 \quad (26)$$

$$\dot{x}_5 = x_6 \quad (27)$$

$$\dot{x}_6 = -\frac{(1-\mu)x_5}{r_1^3} - \frac{\mu x_5}{r_2^3} + u_3 \quad (28)$$

where $x_1 = x, x_2 = \dot{x}, x_3 = y, x_4 = \dot{y}, x_5 = z, x_6 = \dot{z}$

$r_1 = (x_1 + \mu)\hat{x} + x_3\hat{y} + x_5\hat{z}$, $r_2 = (x_1 - (1-\mu))\hat{x} + x_3\hat{y} + x_5\hat{z}$

The cost function is chosen to be a quadratic function of the state and control

$$J = \frac{1}{2}\int_0^\infty [\boldsymbol{x}^T\mathbf{Q}\boldsymbol{x} + \boldsymbol{u}^T\mathbf{R}\boldsymbol{u}]dt \tag{29}$$

where $\boldsymbol{x} = [x_1 \quad x_2 \quad x_3 \quad x_4 \quad x_5 \quad x_6]^T$, $\boldsymbol{u} = [u_1 \quad u_2 \quad u_3]^T$

The weighting functions are chosen to be:

$\boldsymbol{Q} = diag\{q_{11}, q_{22}, q_{33}, q_{44}, q_{55}, q_{66}\}$, $\boldsymbol{R} = diag\{r_{11}, r_{22}, r_{33}\}$

In order to employ the $\theta - D$ method, the condition $f(\mathbf{0}) = \mathbf{0}$ has to be satisfied. However, Eq. (24) has a bias term $-\frac{(1-\mu)(x_1+\mu)}{r_1^3} - \frac{\mu[x_1-(1-\mu)]}{r_2^3}$ which will not go to zero when the states are zero. Therefore, an additional state 's' with stable dynamics is added to the state space in order to absorb the biases.

$$\dot{s} = -\lambda_s s \tag{30}$$

Note that this new variable will not alter the basic dynamics since we treat those bias terms by multiplying and dividing them by s. It is reset to its initial value at each integration step in the simulation. In the simulation, λ_s is set to unity. The augmented state space can be written in a linear-like form:

$$\dot{\tilde{\boldsymbol{x}}} = \boldsymbol{F}(\tilde{\boldsymbol{x}})\tilde{\boldsymbol{x}} + \boldsymbol{g}\boldsymbol{u} \tag{31}$$

where $\tilde{\boldsymbol{x}} = [x_1 \quad x_2 \quad x_3 \quad x_4 \quad x_5 \quad x_6 \quad x_7]^T$ and $x_7 = s$

$$\boldsymbol{F}(\tilde{\boldsymbol{x}}) = \begin{bmatrix} 0 & 1 & 0 & 0 & 0 & 0 & 0 \\ 1 & 0 & 0 & 2 & 0 & 0 & a_{27} \\ 0 & 0 & 0 & 1 & 0 & 0 & 0 \\ 0 & -2 & a_{43} & 0 & 0 & 0 & 0 \\ 0 & 0 & 0 & 0 & 0 & 1 & 0 \\ 0 & 0 & 0 & 0 & a_{65} & 0 & 0 \\ 0 & 0 & 0 & 0 & 0 & 0 & -\lambda_s \end{bmatrix}, \quad \boldsymbol{g} = \begin{bmatrix} 0 & 0 & 0 \\ 1 & 0 & 0 \\ 0 & 0 & 0 \\ 0 & 1 & 0 \\ 0 & 0 & 0 \\ 0 & 0 & 1 \\ 0 & 0 & 0 \end{bmatrix} \tag{32}$$

with $a_{27} = -\frac{(1-\mu)(x_1+\mu)}{r_1^3 s} - \frac{\mu[x_1-(1-\mu)]}{r_2^3 s}$, $a_{43} = 1 - \frac{(1-\mu)}{r_1^3} - \frac{\mu}{r_2^3}$,

$a_{65} = -\frac{(1-\mu)}{r_1^3} - \frac{\mu}{r_2^3}$

In the $\theta - D$ formulation, we choose the factorization of the nonlinear equation (11) in the following form:

$$\dot{\tilde{\boldsymbol{x}}} = \left[\boldsymbol{F}(\tilde{\boldsymbol{x}}_0) + \theta\left(\frac{\boldsymbol{F}(\tilde{\boldsymbol{x}}) - \boldsymbol{F}(\tilde{\boldsymbol{x}}_0)}{\theta}\right)\right]\tilde{\boldsymbol{x}} + \boldsymbol{g}\boldsymbol{u} \tag{33}$$

The advantage of choosing this factorization is that in the $\theta - D$ formulation $\boldsymbol{T}_0$ is solved from $\boldsymbol{A}_0$ and g in (15). If we select $\boldsymbol{A}_0 = \boldsymbol{F}(\tilde{\boldsymbol{x}}_0)$, we would have a good starting point for $\boldsymbol{T}_0$ because $\boldsymbol{A}(\tilde{\boldsymbol{x}}_0)$ retains much more system information than an arbitrary choice of $\boldsymbol{A}_0$ would.

Once $\boldsymbol{A}_0$, g, Q and R are determined, we can follow the algorithm in Section III to get the closed-form solution for $\boldsymbol{T}_0$, $\boldsymbol{T}_1$ and $\boldsymbol{T}_2$. In this simulation, first three terms, i.e. $\mathbf{T}_0, \mathbf{T}_1$ and $\mathbf{T}_2$, in the control equation (18) are used to compute the necessary control. The simulation results show that they are sufficient to achieve satisfactory performance. The final feedback controller takes the form of

$$\boldsymbol{u} = -\mathbf{R}^{-1}\mathbf{g}^T\left[\boldsymbol{T}_0 + \boldsymbol{T}_1(x,\theta)\theta + \boldsymbol{T}_2(x,\theta)\theta^2\right](\tilde{\boldsymbol{x}} - \tilde{\boldsymbol{x}}_r) \tag{34}$$

where $\tilde{\boldsymbol{x}} = [x_r \quad \dot{x}_r \quad y_r \quad \dot{y}_r \quad z_r \quad \dot{z}_r \quad 0]^T$

V. NUMERICAL RESULTS AND ANALYSIS

The initial conditions of the reference trajectory computed in Section II are given by

$x_0 = 87028.50840273$ km, $y_0 = -24739.51262998$ km, $z_0 = -22995.1.974656271$ km

$\dot{x}_0 = -8.985877859$ m/s, $\dot{y}_0 = -121.605674977$ m/s, $\dot{z}_0 = 9.457952755$ m/s

The above data are measured with respect to the L_2 libration point.

$\boldsymbol{Q}$ and $\boldsymbol{R}$ are also tuned to give a satisfactory performance. The values of $\boldsymbol{Q}$ and $\boldsymbol{R}$ are chosen to be

$$\boldsymbol{Q} = diag\{10^{15}, 0, 10^{15}, 0, 10^{15}, 0, 0\}, \boldsymbol{R} = diag\{1,1,1\} \tag{35}$$

$\mathbf{D}_1$ and $\mathbf{D}_2$ in (16) and (17) are chosen according to Remark 3.2:

$$\mathbf{D}_1 = 0.9e^{-10r}\left[\frac{\mathbf{T}_0\mathbf{A}(x)}{\theta}\ \frac{\mathbf{A}^T(x)\mathbf{T}_0}{\theta}\right], \mathbf{D}_2 = 0.9e^{-10r}\left[\frac{\mathbf{T}_1\mathbf{A}(x)}{\theta}\ \frac{\mathbf{A}^T(x)\mathbf{T}_1}{\theta} + \mathbf{T}_1\mathbf{g}\mathbf{R}^{-1}\mathbf{g}^T\mathbf{T}_1\right]$$

Figures 3-6 show the tracking trajectory when the spacecraft enters the orbit at the same initial conditions as the reference orbit. As can be seen, the actual trajectory matches the reference orbit very well. The errors of the X-Y-Z position and velocity between the reference and the achieved are given in Fig. 7. The maximum error lies within 8 km. The three control responses are presented in Fig. 8 and they are physically reasonable. To demonstrate the capability of the $\theta - D$ controller to bring spacecraft deviated from its nominal path back on the reference orbit, a 10% deviation from the initial X-Y-Z position is assumed in the simulation. Fig. 9 compares the achieved trajectory and the reference. The plot shows the trajectory for only 16 days to provide clearer illustration. We can see the $\theta - D$ optimal controller drives the spacecraft back to the reference orbit very quickly. The errors and control history are given in Fig. 10 and Fig. 11 respectively. They are shown in one day time intervals for easier observation. Both decay very quickly. To see the final error and control, the trajectory from day 1 to day 533, which is the last day of the computed reference orbit, is presented in Fig. 12 and Fig. 13. As can be seen, they still remain at the same level as in Fig. 7 and Fig. 8.

VI. CONCLUSIONS

A new suboptimal nonlinear control method, called $\theta - D$ technique, was presented to stationkeep a spacecraft on a reference Lissajous trajectory about the L_2 libration point using continuous thrusting. The nonlinear equation of motion of the CR3BP was used without linearization in this study. This approach gives an approximately closed-form

suboptimal feedback controller and consequently is easy to implement. Numerical results demonstrate the potential of this method for stationkeeping spacecraft with good accuracy. Further studies will be performed by adding disturbances such as solar radiation pressure and measurement noises. More realistic models using ephemerides to locate the Moon, Sun, and Earth will be adopted. Also more results will be presented at the conference by comparing this nonlinear control method with traditional linearization based methods.

REFERENCES

[1] Farquhar, R.W., "The Flight of ISEE-3/ICE: Origins, Mission History, and a Legacy," *AIAA Paper 98-4464,* August 1998.

[2] Farquhar, R.W., "The Control and Use of Libration-Point Satellites," *NASA TR R-346,* September 1970.

[3] Breakwell, J.V., Kamel, A.A., and Ratner, M.J., "Stationkeeping for a Translunar Communication Station," *Celestial Mechanics*, Vol. 10, No. 3, pp. 357-373, 1974.

[4] Simo, C., Gomez, G., Llibre, J., and Martinez, R., "Stationkeeping of a Quasiperiodic Halo Orbit Using Invariant Manifolds," *Proceedings of the Second International Symposium on Spacecraft Flight Dynamics,*, Darmstadt, Germany, pp. 65-70. Oct. 1986.

[5] Howell, K.C. and Pernicka, H.J., "Stationkeeping Method for Libration Point Trajectories," *Journal of Guidance, Control and Dynamics*, Vol. 16, No. 1, pp. 151-157, 1993.

[6] Dwivedi., N.P. "Deterministic Optimal Maneuver Strategy for Multi-Target Missions," *Journal of Optimization Theory and Applications*, Vol. 17, Nos. 1/2, pp. 133-153, 1975.

[7] Cielaszyk, D. and Wie, B. "New Approach to Halo Orbit Determination and Control," *Journal of Guidance, Control and Dynamics*, Vol. 19, No. 2, pp. 2660-273, 1996.

[8] Dunham, D.W. and Roberts, C.E., "Stationkeeping Techniques for Libration-Point Satellites," *Journal of the Astronautical Sciences*, Vol. 49, No. 1, pp. 127-144, 2001.

[9] Rahmani, A., Jalali, M.A., Pourtakdoust, S.H., "Optimal Approach to Halo Orbit Control," *AIAA Guidance, Navigation, and Control Conference and Exhibit*, Austin, Texas, Aug. 11-14, 2003.

[10] Howell, K.C. and Pernicka, H.J., "Numerical Determination of Lissajous Trajectories in the Restricted Three-Body Problem," *Celestial Mechanics*, Vol. 41, pp. 107-124, 1988.

[11] Bryson, Jr., A.E. and Ho, Y-C., *Applied Optimal Control*, Hemisphere Publishing Corporation, 1975.

[12] Xin, Ming and S.N. Balakrishnan, "A New Method for Suboptimal Control of A Class of Nonlinear Systems," *Proceedings of IEEE Conference on Decision and Control*, Las Vegas, Nevada, Dec. 10-13, 2002.

[13] Xin, M., Balakrishnan, S.N., Stansbery, D.T. and Ohlmeyer, E.J., "Nonlinear Missile Autopilot Design with Theta-D Technique," *AIAA Journal of Guidance, Control and Dynamics*, accepted and in print, 2004.

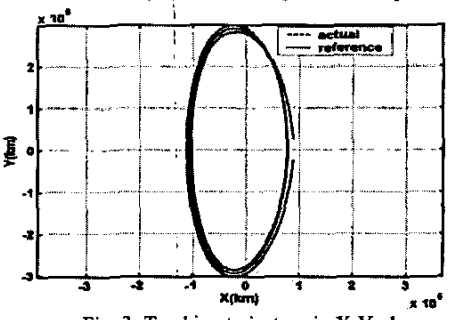

Fig. 3: Tracking trajectory in X-Y plane

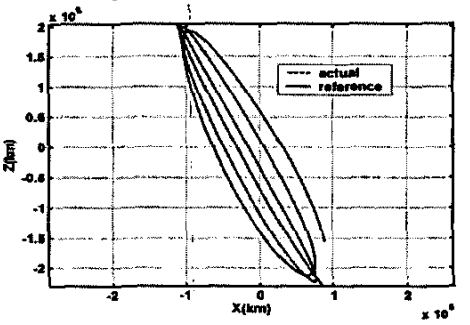

Fig. 4: Tracking trajectory in X-Z plane

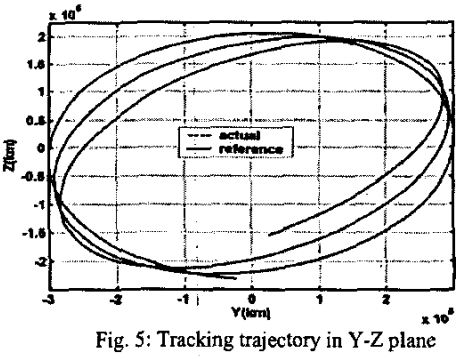

Fig. 5: Tracking trajectory in Y-Z plane

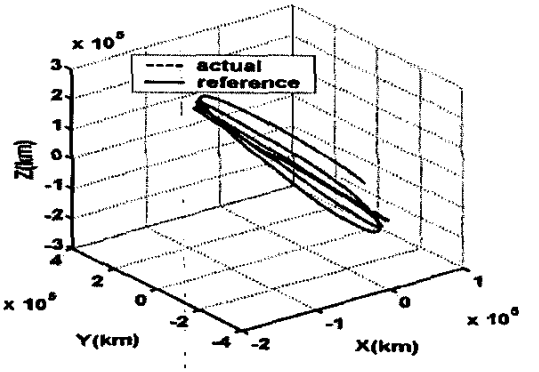

Fig. 6: Tracking trajectory in X-Y-Z view

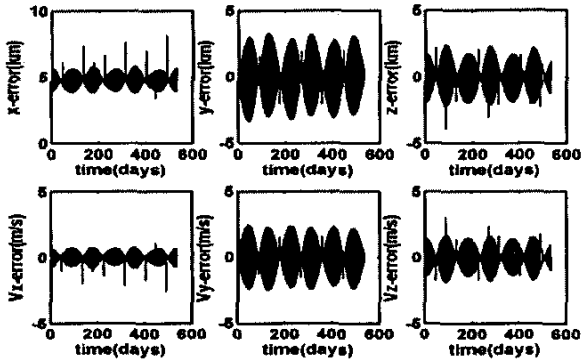

Fig. 7: Tracking error of positions and velocities

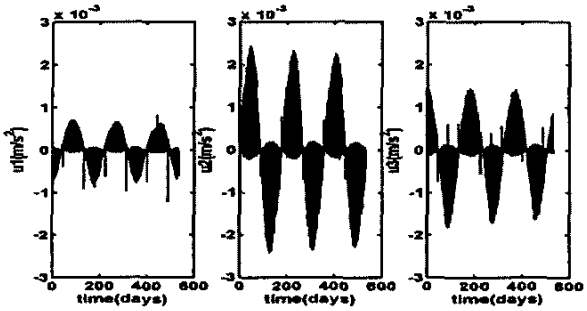

Fig. 8: Control usage

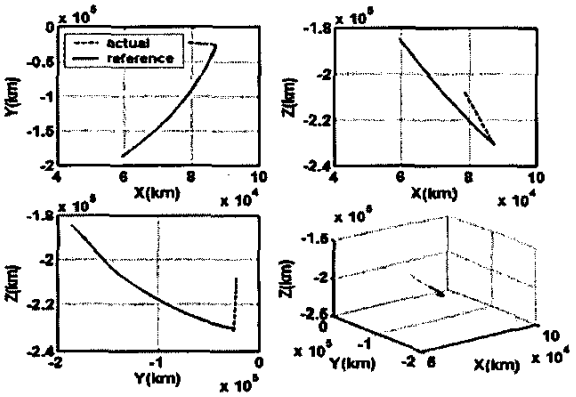

Fig. 9: Tracking trajectory with 10% initial deviations

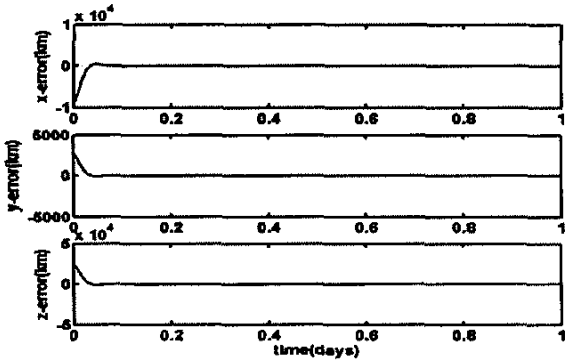

Fig. 10: Tracking error with 10% initial deviation

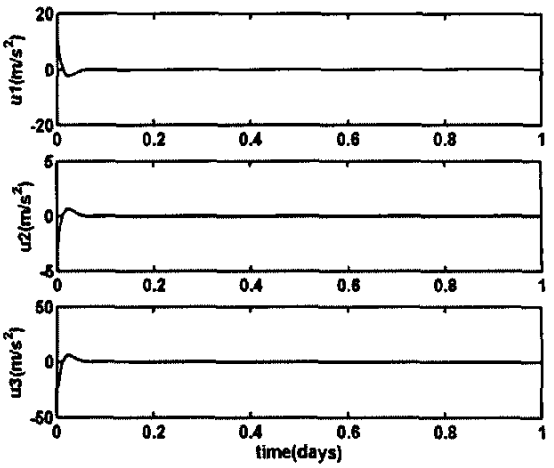

Fig. 11: Control with 10% initial deviation

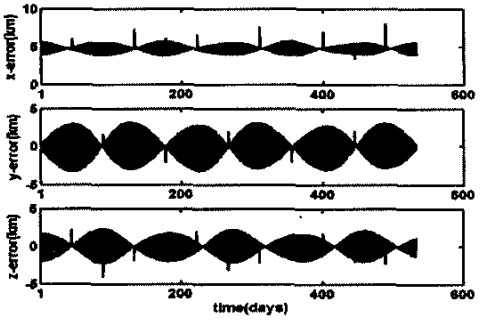

Fig. 12: Tracking error with 10% initial deviation (1-533 days)

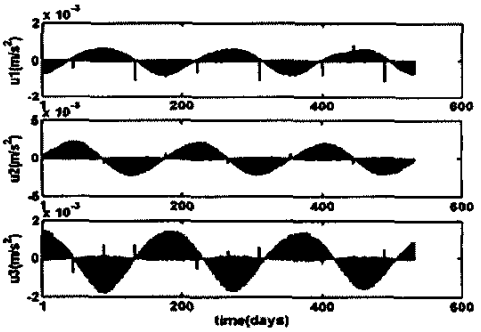

Fig. 13: Control with 10% initial deviation (1-533 days)